引用格式：MENG Fanlin, SU Shi, ZHANG Guoyu, et al. Design Method of Solar Radiation Simulation Optical System with High Energy Utilization Rate[J]. Acta Photonica Sinica, 2021, 50(12):1222003
孟凡琳,苏拾,张国玉,等.高能量利用率太阳辐射模拟光学系统设计[J].光子学报,2021,50(12):1222003

高能量利用率太阳辐射模拟光学系统设计

孟凡琳[1],苏拾[1,2],张国玉[1,2],张健[1,2],刘石[1,2],孙高飞[1,2],彭浩文[1]
(1 长春理工大学 光电工程学院,长春 130022)
(2 吉林省光电测控仪器工程技术研究中心,长春 130022)

摘 要:针对以往大型太阳模拟器结构复杂、能量利用率低、均匀性较差等的不足,提出了高能量利用率太阳辐射模拟光学系统设计方法。基于真实氙灯光源的发光特性设计椭球聚光镜,通过添加球面反光镜,利用组合聚光系统提高能量利用率,依据光瞳匹配原则设计光学积分器,利用边缘消杂光法提高辐照均匀性。仿真分析可知:组合聚光系统比单个椭球聚光镜能量利用率提高21.2%,利用边缘消杂光法比边缘补偿法辐照均匀性提高4%。实验结果表明:工作距离20 m,辐照面直径Φ2 m时,最大辐照度为1 363.1 W·m^{-2},辐照不均匀度为±4.5%,实现大面积、高能量利用率的太阳光辐射模拟,为航天领域太阳敏感器地面半物理仿真与测试提供有效手段。

关键词:太阳辐射模拟;高能量利用率;大面积;组合聚光系统;边缘消杂光法
中图分类号:O436 **文献标识码**:A **doi**:10.3788/gzxb20215012.1222003

Design Method of Solar Radiation Simulation Optical System with High Energy Utilization Rate

MENG Fanlin[1], SU Shi[1,2], ZHANG Guoyu[1,2], ZHANG Jian[1,2], LIU Shi[1,2], SUN Gaofei[1,2], PENG Haowen[1]
(1 *College of Optoelectronic Engineering, Changchun University of Science and Technology, Changchun* 130022, *China*)
(2 *Jilin Province Engineering Research Center of Optical Measurement and Control Instrumentation, Changchun* 130022, *China*)

Abstract: Aiming at the disadvantages of large-scale solar simulators in the past, such as complex structure, low energy utilization rate and poor uniformity, a design method of solar radiation simulation optical system with high energy utilization rate was proposed. The ellipsoid condenser was designed based on the luminous characteristics of the real xenon lamp. By adding a spherical reflector, the combined condenser system was used to improve the energy utilization rate. The optical integrator was designed according to the principle of pupil matching. The irradiation uniformity was improved by the edge elimination method. The simulation results suggest that the energy utilization rate of the combined condenser system is 21.2% higher than that of the single ellipsoid condenser. The irradiation uniformity of the edge elimination method is 4% higher than that of the edge compensation method. The experimental results suggest that the working distance is 20 m, irradiation surface diameter is Φ2 m, maximum irradiance is 1 363.1 W·m^{-2}, non-uniformity is ±4.5%. It has realized large-area, high-energy utilization

Foundation item: Science and Technology Plan Project of Jilin Province (No. 20190302064GX)
First author: MENG Fanlin (1997—), female, M.S. degree candidate, mainly focuses on solar simulation technology. Email:mengfl6@163.com
Supervisor (Contact author): SU Shi (1978—), male, professor, Ph.D. degree, mainly focuses on solar simulation technology and meteorological solar radiation instrument verification technology. Email:sushi@cust.edu.cn
Received: Apr.28,2021; **Accepted**: Aug.9,2021

rate solar radiation simulation, which provided an advanced means for semi-physical simulation and testing of solar sensors in space field.

Key words: Solar radiation simulation; High energy utilization rate; Large area; Combined condenser system; Edge elimination method

OCIS Codes: 220.4830; 080.2740; 080.3620; 080.4298; 120.3620; 120.4570

0 Introduction

Solar simulator is a kind of test equipment and calibration equipment that simulates solar radiation with artificial light source[1-2]. It has been widely used in the field of space semi-physical simulation and testing of solar sensors on the ground, attitude control of satellite space flight, thermal balance test of spacecraft, and probe test in lunar exploration project[3-5].

In order to realize the simulation of solar irradiation with large area spots, most of the large-scale solar simulators currently use off-axis optical system, and several xenon lamps are used as the array of light sources[6-9]. However, off-axis solar simulator has large volume, complex structure, high difficulty in installation and adjustment, and high manufacturing cost. In addition, the use of multiple xenon lamp arrays can improve the irradiation intensity, but the energy utilization rate is low, and the irradiation uniformity is poor. Therefore, in order to meet the continuous development of aerospace engineering, on the basis of low cost and high uniformity, it is imperative to research a kind of optical system which can achieve long-distance, large area and high energy utilization of solar irradiation simulation.

In addition, the current research on solar simulator is mostly focused on how to improve the irradiation uniformity, and there are few studies on how to improve the energy utilization rate. For example, PARUPUDIA R V and others designed parabolic mirrors to effectively improve the irradiation uniformity of the solar simulator[10]. To improve the spatial uniformity of the concentrating solar simulators, XIAO Jun and others introduced a concept of non-coaxial deflection angle to the typical ellipsoidal reflectors[11]. LV Tao and others studied the ellipsoid converging lens with variable curvature[12] and optical integrator for the number and shape of the element lens[13] to improve irradiation uniformity.

In some fields, combined condenser systems are used to improve the energy utilization rate. For example, MENG Xiangxiang and others designed a trapezoidal secondary concentrator to improve the conversion efficiency of laser cells[14]. GUO Qibo designed a combined LED condenser that includes a reflective cup to improve the efficiency of light use[15]. YANG Chen designed a combined face concentrating device to achieve a high flux of concentrated light at a small aperture outlet[16]. WU Qing and others designed a kind of high reflectivity light distribution bulb with the combination of ellipse and multi-curved surface, which can effectively improve the focusing effect and make full use of energy[17]. Based on the above experience, the combined condenser system is considered to be applied to the solar simulator to improve the energy utilization rate of the solar simulator.

Aiming at the problems of high cost, complex structure, low energy utilization rate and poor irradiation uniformity of the current large-scale solar simulator, a solar radiation simulation optical system with high energy utilization rate is designed. The combined condenser system is adopted to improve the energy utilization rate and the edge compensation method is used to improve the irradiation uniformity. The simulation of solar irradiation with high energy utilization rate and high uniformity is realized.

1 General layout of a solar radiation simulation optical system with high energy utilization rate

The solar radiation simulation optical system with high energy utilization rate consists of a high-power xenon lamp light source, a concentrating system and a homogenizing system, as shown in Fig. 1.

In order to improve the energy utilization rate, the concentrating system adopts the combined condenser system, which is composed of an ellipsoidal condenser and a spherical reflector. The homogenizing system uses the optical integrator to homogenize the convergent Gaussian radiation distribution and emit it at a certain divergence angle[18]. The high-power xenon lamp is located at the first focus of the ellipsoid condenser. The light

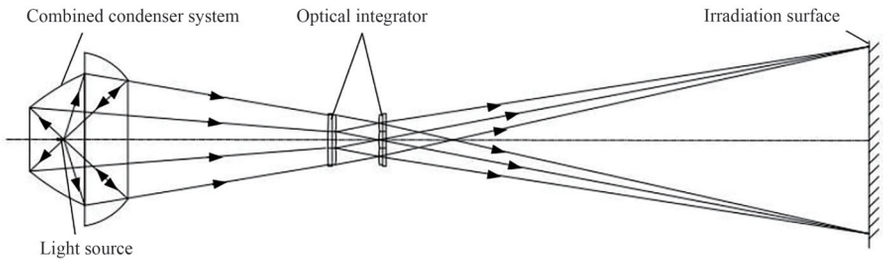

Fig.1 Solar radiation simulation optical system

emitted by the light source is reflected and converged to the second focal plane by the combined condenser system, and then homogenized by the homogenizing system. Finally, a large area, high irradiance and high uniformity of solar irradiation simulation spot is formed.

2 Optical system design

2.1 Combined condenser system design

2.1.1 *Ellipsoid condenser design*

In previous designs, the xenon lamp was ideally used as a point light source and a single ellipsoid condenser was used to collect the light. However, the real xenon light source obeys a certain luminous intensity and angular distribution, limited by the containment angle, there will be a large amount of stray light that cannot be used. In order to avoid the energy loss beyond the containment angle, eliminate stray light and improve the energy utilization rate, a combined condenser system composed of ellipsoid condenser and spherical reflector is adopted[19].

The xenon arc is simplified to a cylindrical model with length l_0 and diameter d_0. The light path principle of the ellipsoid condenser is shown in Fig. 2. The light emitted by the light source at the first focus converges to the second focal plane after reflection by the ellipsoid condenser. Since the xenon arc has a certain volume, it will form a wide range of light spot.

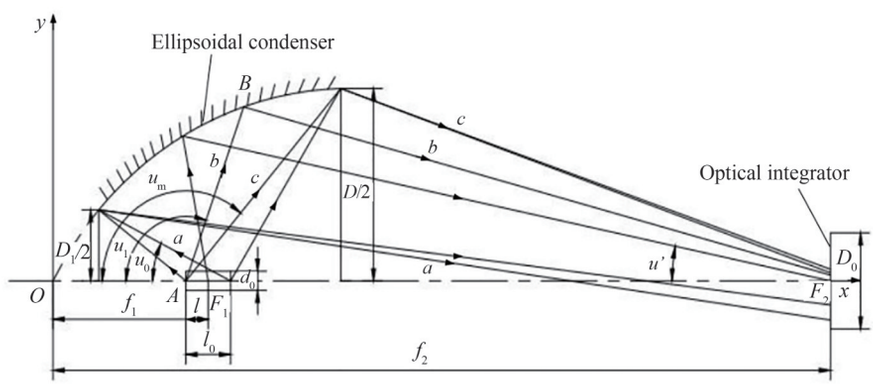

Fig.2 The light path principle of the ellipsoid condenser

The x-axis is the optical axis, F_1 is the first focus, F_2 is the second focus, D_1 is the rear opening diameter of the condenser, D is the front opening diameter of the condenser, D_0 is the optical aperture of the optical integrator, angle u is the aperture angle of incident beam, angle u' is the aperture angle of the outgoing beam, angle u_0 is the rear opening aperture angle corresponding to the luminous point on the shaft, angle u_m is the front opening aperture angle corresponding to the luminous point on the shaft, angle u_1 is the aperture angle corresponding to the beam b emanating from the luminous point $A(f_1-l,0)$ on the axis, l is the distance from point A to point F_1, beams a and c are the beams emitted from the rear opening and the front opening respectively.

Let the ellipsoid equation be

$$y^2=4\frac{f_1f_2}{f_1+f_2}x-\left(1-\left(\frac{f_2-f_1}{f_2+f_1}\right)^2\right)x^2 \tag{1}$$

The range of the effective containment angle of the ellipsoid condenser should match the light distribution curve of the xenon lamp to maximize the energy utilization. The luminous range of the xenon lamp light distribution curve is 30°~135°. In order to make full use of the light energy, the reflection area of the ellipsoid condenser should contain this area. D_1 is determined by u_0, and D is determined by u_m. According to Eq. (2) and Eq. (3), D_1 and D can be obtained,

$$\left(\frac{D_1}{2}\right)^2=4\frac{f_1f_2}{f_1+f_2}\left(f_1+\frac{l_0}{2}-\frac{D_1}{2\tan u_0}\right)-\left(1-\left(\frac{f_2-f_1}{f_2+f_1}\right)^2\right)\left(f_1+\frac{l_0}{2}-\frac{D_1}{2\tan u_0}\right)^2 \tag{2}$$

$$\left(\frac{D}{2}\right)^2=4\frac{f_1f_2}{f_1+f_2}\left(f_1-\frac{l_0}{2}-\frac{D}{2\tan u_m}\right)-\left(1-\left(\frac{f_2-f_1}{f_2+f_1}\right)^2\right)\left(f_1-\frac{l_0}{2}-\frac{D}{2\tan u_m}\right)^2 \tag{3}$$

After D is determined, the depth H of the ellipsoid condenser is calculated

$$H=\frac{f_1+f_2}{2}-\frac{f_1+f_2}{2\sqrt{f_1f_2}}\sqrt{f_1f_2-\left(\frac{D}{2}\right)^2} \tag{4}$$

In addition to the light emitted by the luminescent point at F_1 converging to F_2 for imaging, the light emitted by other luminescent points outside F_1 at different incident angles is reflected, and the position on the second focal plane is a function of the incident Angle. Only the actual calculation of the light can determine the accurate position of the image point. If the light from $A(f_1-l,0)$ on the xenon arc axis intersects the ellipsoid at the point $B(x_0,y_0)$, when the aperture Angle u_l is given, the incident ray equation is,

$$y=\tan(\pi-u_l)\left[x-(f_1-l)\right] \tag{5}$$

$B(x_0,y_0)$ can be obtained according to Eq. (1) and Eq. (4). According to the law of reflection, the angle of reflection is equal to the angle of incidence, so we can figure out the slope of the reflected ray,

$$k=\frac{y_0\left[2\left(x-\left(f_1-l\right)\right)t+t^2-y_0^2\right]}{2ty_0^2-\left(x-\left(f_1-l\right)\right)t^2+\left(x-\left(f_1-l\right)\right)y_0^2} \tag{6}$$

where $t=2\frac{f_1f_2}{f_1+f_2}-\left(1-\left(\frac{f_2-f_1}{f_2+f_1}\right)^2\right)x_0$, then the reflected light equation is

$$y-y_0=k\left(x-x_0\right) \tag{7}$$

When $x=f_2$, the intersection of the light emitted by $A(f_1-l,0)$ with the second focal plane after being reflected by the ellipsoid can be calculated. When the light is incident at the aperture angle u_{lm}, the y value of the intersection point with the second focal plane after reflection from the ellipsoid condenser is the maximum, so that the spot diameter at the second focal plane can be determined. In order to ensure a high energy utilization rate, the optical aperture D_0 of the field lens set of the optical integrator is equal to the spot diameter at the second focal plane.

$$D_0=2k\left(f_2-x_0\right)+y_0 \tag{8}$$

2.1.2 *Spherical reflector design*

In order to improve the energy utilization rate, the optical axes of the spherical reflector and the ellipsoid condenser coincide, and the light from the edge of the ellipsoid condenser can enter the spherical reflector, so that the light beyond the containment angle can be used for a second time. According to the optical principle of the sphere, the light emitted by the xenon lamp located at the center of the sphere is reflected by the spherical reflector, and the light will be reflected back to the center of the sphere without spherical aberration and loss. Using this principle, the center of the spherical reflector coincides with the first focus F_1 of the ellipsoid condenser. The direct light emitted by the xenon lamp is reflected back to F_1 through the spherical reflector, and then converged to F_2 through the ellipsoid condenser, which reduces the energy loss and improves the energy utilization rate.

The external dimensions of the spherical reflector are shown in Fig. 3.

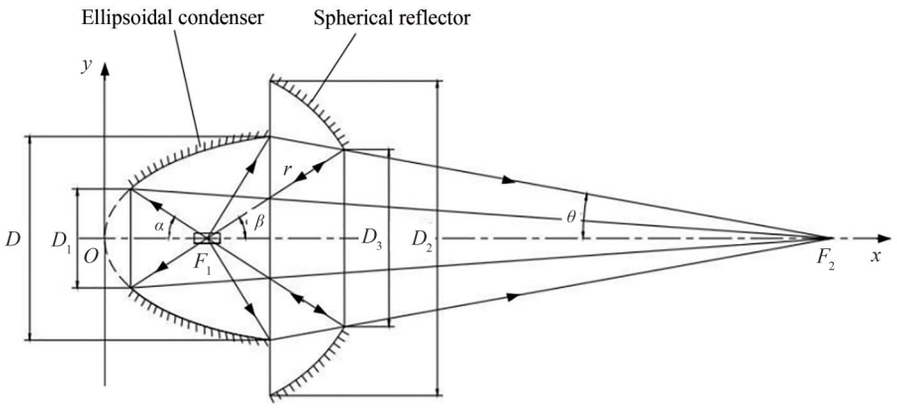

Fig.3 The external dimensions of the spherical reflector

The spherical equation is

$$(x-f_1)^2+y^2=\left(\frac{f_2-f_1}{180^\circ-\theta-\beta}\theta\right)^2 \tag{9}$$

The diameter D_2 of the back opening of the spherical mirror and the diameter D_3 of the front opening are

$$D_2=2\sqrt{r^2-\left(f_2-f_1-\frac{D}{2\tan\theta}\right)^2} \tag{10}$$

$$D_3=2r\sin\beta \tag{11}$$

where $\beta=\alpha$, α is the aperture angle of the rear opening corresponding to F_1, and θ is the aperture angle of the outgoing beam corresponding to the edge rays of the ellipsoid condenser.

2.2 Homogenizing system design

The homogenization system adopts an optical integrator to homogenize the Gaussian radiation distribution and emit it at a certain divergence angle. The optical integrator is composed of a field lens group L_F, a projection lens group L_P and two additional lenses (L_1 and L_2), as shown in Fig. 4. The field lens group is placed at the second focal plane, and the light emitted by the light source is divided into multiple images by L_1 and L_F, and projected to the corresponding projection lens group respectively. The images are superimposed to the irradiation surface by L_P and L_2, and the irradiation uniformity is improved by the way of light segmentation, superposition and symmetric compensation.

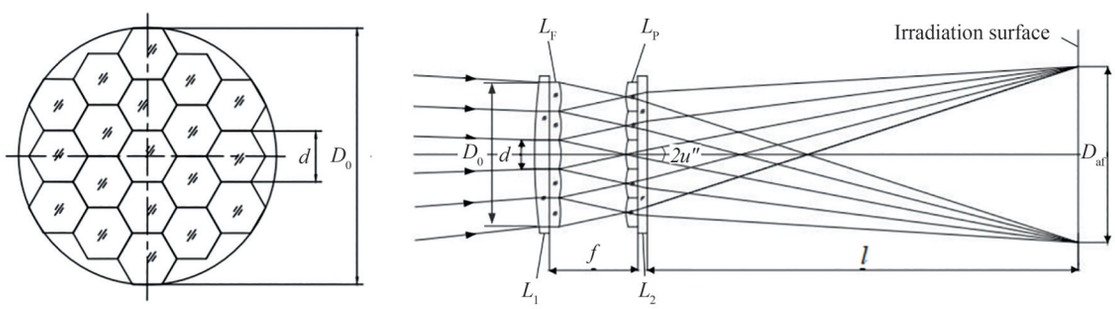

(a) Element lens arrangement (b) Optical path schematic diagram

Fig.4 The structure of optical integrator

The field lens group and the projection lens group are composed of multiple element lenses arranged symmetrically according to the center. The aperture and focal length of the two groups of element lenses are the same, and they are in the focal plane of each other. If the number of element lenses is too small, the evenness effect cannot be guaranteed. In excess, the uniformity is affected by machining errors. Considering the

processing difficulty and the effect of uniform light, 19 regular hexagonal element lenses are selected. The diameter of the inner circle of the element lens d is

$$d=\frac{D_0}{N} \tag{12}$$

where N is the number of element lenses contained in the diameter of the outer tangential circle of the optical integrator.

In order to improve energy utilization rate and reduce stray radiation of optical system, it is necessary to consider the factor that the relative aperture of the condenser system matches the relative aperture of the element lens of optical integrator. According to the principle of pupil matching, the following relation is established to calculate the focal length f of the element lens,

$$\frac{D}{f_2-H}=\frac{d}{f} \tag{13}$$

The whole optical integrator system is represented by six matrices, the first matrix is incident matrix, the next four are field mirror matrix, projection mirror matrix, and the last one is additional mirror matrix. The incident angle of the rays is u', and the exit angle is u''. The focal length of the two groups of element lenses is the same, $f_{L_F}=f_{L_P}=f$. According to Eq. (14), the irradiation surface diameter D_{af} can be obtained.

$$\begin{pmatrix} D_{af} \\ u'' \end{pmatrix}=\begin{pmatrix} 1 & l \\ 0 & 1 \end{pmatrix}\begin{pmatrix} 1 & 0 \\ -\dfrac{1}{l} & 1 \end{pmatrix}\begin{pmatrix} 1 & 0 \\ -\dfrac{1}{f_{L_P}} & 1 \end{pmatrix}\begin{pmatrix} 1 & f \\ 0 & 1 \end{pmatrix}\begin{pmatrix} 1 & 0 \\ -\dfrac{1}{f_{L_F}} & 1 \end{pmatrix}\begin{pmatrix} d \\ u' \end{pmatrix} \tag{14}$$

When the working distance l and divergence Angle α are given, the optical aperture D_0' of the projection lens group of the optical integrator can be calculated.

$$D_0'=D_{af}-l\tan\alpha \tag{15}$$

The irradiance at the edge of the irradiation surface of the solar simulator is usually lower than the central irradiance. The edge compensation method is usually adopted, that is, several small triangular lenses are added to the edge of the optical integrator to improve the edge irradiance, so as to improve the irradiation uniformity. However, considering the processing cost, an edge elimination aperture is designed according to the element lens array to intercept the edge light and ensure that the light can only pass through the element lens to improve the irradiation uniformity. Edge compensation method and edge elimination method are shown in Fig. 5 and Fig. 6.

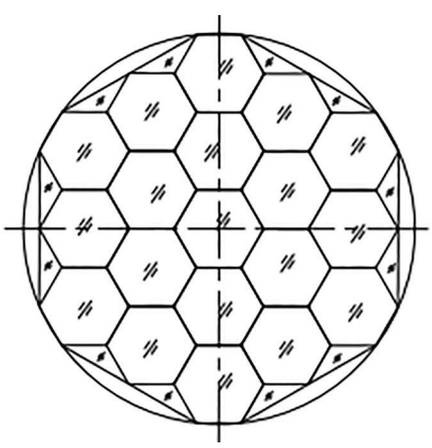

Fig. 5 Edge compensation method

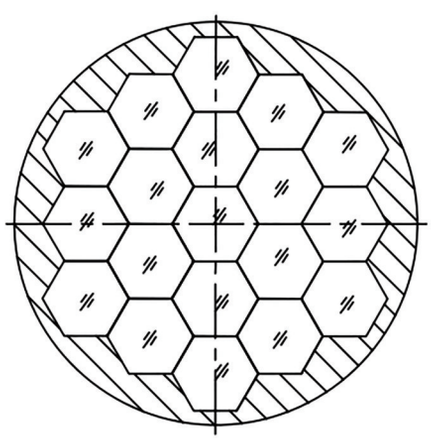

Fig. 6 Edge elimination method

3 Simulation and experiment

3.1 Simulation analysis

The working distance of the solar radiation simulator optical system is 20 m, and the diameter of the

irradiation surface is Φ2 m. The optical parameters are shown in Table 1.

Table 1 Optical system parameter

M_0/(×)	f_1/mm	f_2/mm	D_1/mm	D/mm	D_2/mm	D_3/mm	D_0/mm	d/mm	f/mm	α/(°)
23	57.35	1319	61.28	301.58	506.4	268.7	225	45	450	5.07

3.1.1 *Comparison of energy utilization rate between single ellipsoid condenser and combined condenser system*

A single ellipsoid condenser and a combined condenser system were modeled and simulated by using LightTools software. The receiver was placed at the second focal plane, and the radiation flux was set as 20 000 W. The energy utilization rate of the two was compared. The simulation light path is shown in Fig. 7, and the energy utilization rate comparison is shown in Fig. 8.

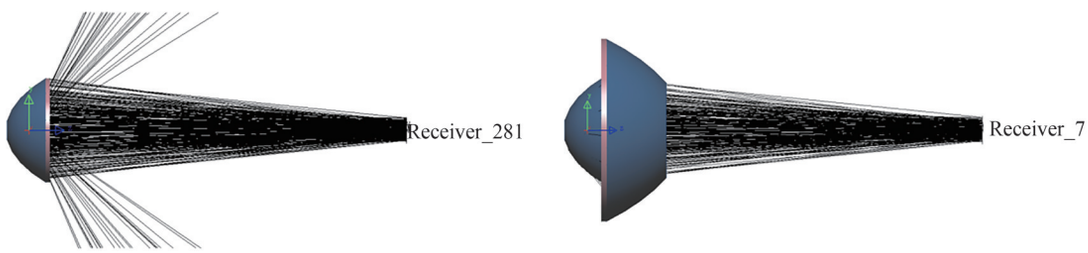

(a) Single ellipsoid condenser (b) Combined condenser system

Fig. 7 Simulation light path diagram

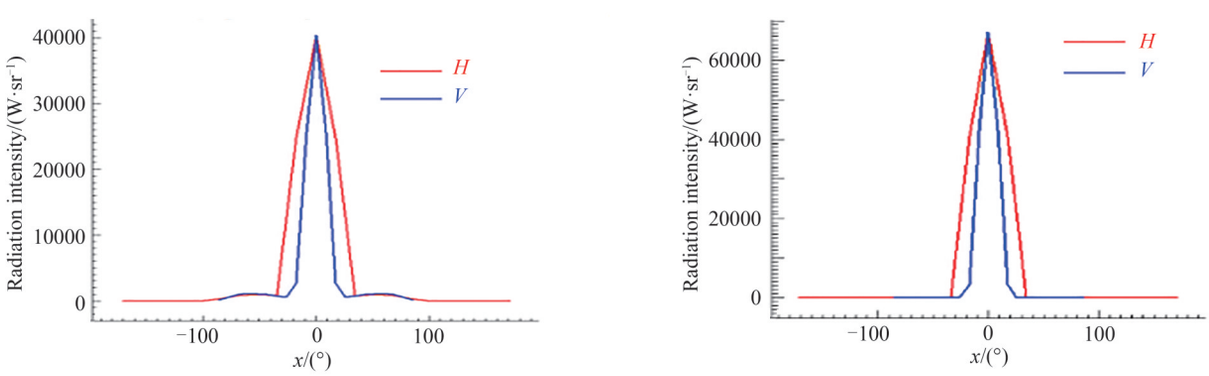

(a) Single ellipsoid condenser (b) Combined condenser system

Fig. 8 Energy utilization rate comparison

As can be seen from Fig. 7 and Fig. 8, the single ellipsoid condenser has a large amount of stray light that cannot be utilized, and the combined condenser system eliminates the stray light. At the second focal plane, the single ellipsoid condenser receives 10 131 W of energy, and the energy utilization rate is 50.66%. The combined condenser system receives 14 372 W of energy, and the energy utilization rate is 71.86%. The energy utilization rate is increased by 21.2%.

3.1.2 *Comparison of irradiation uniformity between uncompensated optical integrator, edge compensation method and edge elimination method*

LightTools software was used to model and simulate the optical integrator, and the irradiation uniformity of uncompensated, edge compensation method and edge elimination method was compared. The simulation model is shown in Fig. 9, and the irradiation uniformity comparison is shown in Fig. 10.

As can be seen from Fig. 10, when the optical integrator is uncompensated, the irradiance of the edge is lower than that of the center. The edge irradiance is improved when the edge compensation method is used. The irradiation uniformity is improved obviously by using the edge elimination method. Compared with uncompensated method, the improvement is 8.4%, and the improvement is 4% compared with edge

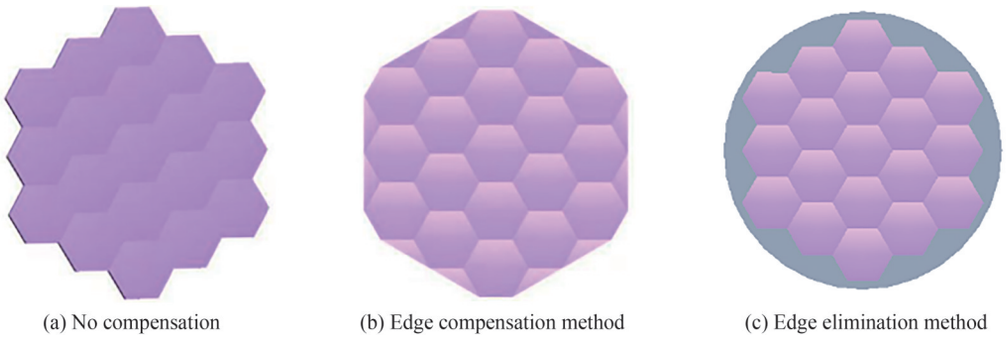

Fig. 9 Simulation model of optical integrator

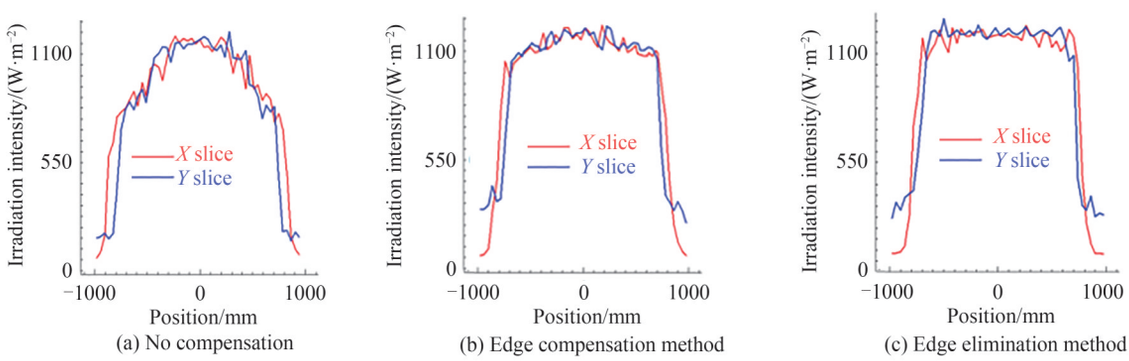

Fig. 10 Comparison of irradiation uniformity

compensation method.

3.1.3 *Integrated optical system simulation*

LightTools software was used to simulate the integrated optical system by combining the modeling of the combined condenser system and optical integrator. The simulation model is shown in Fig. 11, and the

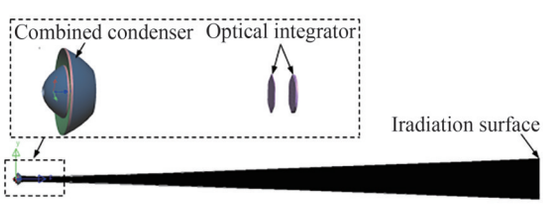

Fig. 11 Optical system simulation model

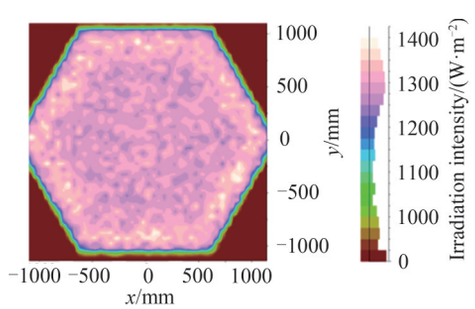

Fig. 12 Simulation results of irradiation uniformity

simulation results of irradiation uniformity are shown in Fig. 12.

The calculation formula of irradiation non-uniformity is[20]

$$\varepsilon = \pm \frac{E_{\max} - E_{\min}}{E_{\max} + E_{\min}} \times 100\% \tag{16}$$

where ε is the irradiation non-uniformity, $E_{\max}$ is the maximum irradiance and $E_{\min}$ is the minimum irradiance.

As can be seen from Fig. 12, the working distance is 20 m, the diameter of the irradiation surface is 2 m, the maximum irradiance is 1 372.6 W·m^{-2}, and the minimum irradiance is 1 258.5 W·m^{-2}. According to Eq. (16), the simulation result of irradiation non-uniformity can be calculated as $\pm$4.3%.

3.2 Experimental verification

The working distance and the diameter of the irradiation surface of the solar radiation simulator with high energy utilization rate were tested by using the laser anomaly calibration system. When the working distance is 20 m, the diameter of the irradiation surface is Φ2 m. The uniformity was measured and evaluated with FZ-A

solar irradiance meter from Beijing Normal University Photoelectric Instrument Factory. The wavelength range of FZ-A solar irradiance meter is (400～1 000) nm, the minimum resolution is 10^{-4} mW·cm^{-2} and the upper limit of measurement is 199.9 mW·cm^{-2}.

The short-arc xenon lamp was lit, and the FZ-A solar irradiance meter was placed on the effective working irradiation surface of the solar simulator, with the photosensitive surface facing the mirror cylinder of the solar simulator. After the light source was stabilized, 41 sampling points were selected on the effective irradiation surface to conduct the irradiation non-uniformity test, and repeated measurements were made for several times to eliminate the errors caused by light intensity instability. The distribution of test sampling points is shown in Fig. 13, the test results of irradiation non-uniformity are shown in Fig. 14, and the experimental

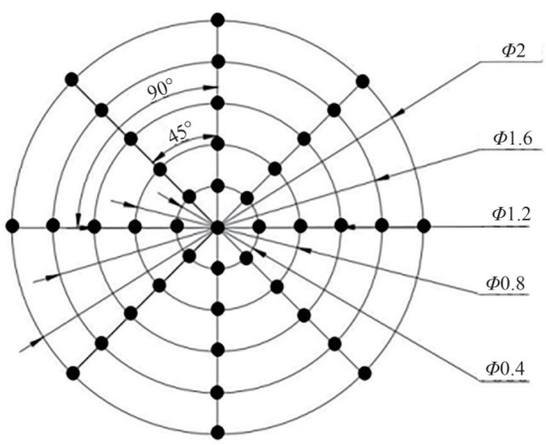

Fig. 13 Distribution of test sampling points

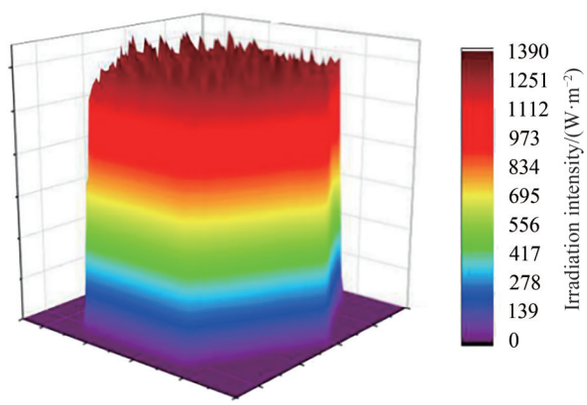

Fig. 14 Test results of irradiation non-uniformity

Table 2 Experimental data of irradiance

Distance from the center point/m	Angle of rotation about the center point/(°)			
	0	45	90	135
−1	1 250.2	1 249.8	1 251.2	1 252.5
−0.8	1 253.7	1 259.6	1 261.8	1 257.4
−0.6	1 263.4	1 263.3	1 270.6	1 245.4
−0.4	1 245.5	1 257.4	1 285.3	1 278.7
−0.2	1 288.7	1 298.5	1 296.4	1 287.4
0	1 363.1	/	/	/
0.2	1 312.5	1 308.7	1 311.5	1 309.2
0.4	1 258.4	1 269.8	1 295.5	1 298.8
0.6	1 268.5	1 294.3	1 287.3	1 287.4
0.8	1 273.8	1 288.5	1 269.7	1 270.3
1	1 261.4	1 274.6	1 263.6	1 268.9

data of irradiance are shown in Table 2.

The maximum irradiance and minimum irradiance in the effective irradiation surface measured by the experiment are 1 363.1 W·m^{-2} and 1 245.4 W·m^{-2} respectively. According to Eq. (16), the irradiation non-uniformity can be calculated to be ±4.5%.

4 Conclusion

A design method of solar radiation simulation optical system with high energy utilization rate using a single high power xenon lamp as light source was proposed. Based on the luminous characteristics of real xenon lamp, the ellipsoid condenser was designed. On this basis, the combined condenser system was used to improve the energy utilization rate by adding a spherical reflector. The optical integrator was designed according to the

principle of pupil matching and the irradiation uniformity was improved by using the edge elimination method. The simulation results show that the energy utilization rate of the combined condenser system is increased by 21.2% compared with that of a single ellipsoid condenser. Compared with the edge compensation method, the irradiation uniformity is improved by 4% by using the edge elimination method of optical integrator. The experimental results show that the working distance is 20 m, the diameter of the irradiation surface is Φ2 m, the maximum irradiance is 1 363.1 W·m^{-2}, and the irradiation non-uniformity is ±4.5%. It has broken the shortcomings of the large size, complex structure, low energy utilization rate and poor uniformity of the previous large-scale solar simulator, and provided an advanced means for the ground semi-physical simulation and testing of the solar sensor in the field of space.

References

[1] RANGA V P, HARJIT S, MARIA K. Sun simulator for performance assessment of solar photovoltaic cells[J]. Energy Procedia, 2019, 161: 376-384.

[2] MENG Qinglong, LI Yanpeng, GU Yaxiu. Dynamic mesh-based analysis of dynamic irradiance characteristics of solar simulator[J]. Optik, 2015, 126: 4658-4664.

[3] SIDDIQUI R, KUMAR R, JHA G K. Comparison of different technologies for solar PV (Photovoltaic) outdoor performance using indoor accelerated aging tests for long term reliability[J]. Energy, 2016, 107: 550-561.

[4] ZAINI H, YOO J K, PARK S, et al. Indoor calibration method for UV index meters with a solar simulator and a reference spectroradiometer[J]. International Journal of Metrology and Quality Engineering, 2016, 7(1): 101.

[5] TAWFIK M, TONNELLIER X, SANSOM C. Light source selection for a solar simulator for thermal applications: a review[J]. Renewable and Sustainable Energy Reviews, 2018, 90: 802-813.

[6] LI Xian, CHEN Jialing, LIPINSKI W, et al. A 28 kWe multi-source high-flux solar simulator: design, characterization, and modeling[J]. Solar Energy, 2020, 211: 569-583.

[7] BAZZI A M, KLEIN Z, SWEENEY M, et al. Solid-state light simulator with current-mode control[C]. Applied Power Electronics Conference & Expositio, 2011, New York: IEEE, 11931227.

[8] LIU Shi, ZHANG Guoyu, SUN Gaofei, et al. Design of optical integrator for solar simulator[J]. Acta Photonica Sinica, 2013, 41(4): 467-470.

[9] GILL R, BUSH E, HAUETER P, et al. Characterization of a 6kW high-flux solar simulator with an array of xenon arc lamps capable of concentrations of nearly 5000 suns[J]. Review of Scientific Instruments, 2015, 86(12): 021005.

[10] PARUPUDIA R V, SINGHA H, KOLOKOTRONI M. Simulator for indoor performance assessment of solar photovoltaic cells[J]. Energy Procedia, 2019, 161: 376-384.

[11] XIAO Jun, WEI Xiudong, GILABER R N, et al. Design and characterization of a high-flux non-coaxial concentrating solar simulator[J]. Applied Thermal Engineering, 2018,145:201-211.

[12] LV Tao, ZHANG Jingxu, FU Donghui, et al. A deformed ellipsoid condenser beneficial to the uniformity of the solar simulator[J]. Acta Optica Sinica, 2013, 33(12): 253-257.

[13] LV Tao, FU Donghui, CHEN Xiaoyun, et al. Effect of optical intergrator element lenses′ number and shape on the lighting uniformity of solar simulator[J]. Journal of Optoelectronics·Laser, 2014, 25(10): 1849-1853.

[14] MENG Xiangxiang, SHEN Jingshi, SHI Dele, et al. Secondary concentration of laser wireless power transmission receiving system[J]. Infrared and Laser Engineering, 2017, 46(7): 76-80.

[15] GUO Qibo. A combined LED condenser lens: China, CN201320040916.0[P]. 2013-07-24.

[16] YANG Chen, ZENG Ruimin. A combined face body light gathering device: China, CN201920324873.6[P]. 2019-08-23.

[17] WU Qing, LIU Songyue, DU Chuande. High reflectivity light distribution bulb with elliptic and multi-curved combination concentrating light and a manufacturing method thereof: China, CN201510752623.9[P]. 2016-05-25.

[18] SUN Gaofei, ZHANG Guoyu, LIU Shi, et al. Designing an optical system for a high precision solar simulator for meteorological application[J]. Journal of Optical Technology, 2017, 84(8): 59-63.

[19] ZHANG Ran, ZHANG Guoyu, LIANG Jing, et al. Design on composite condenser of solar simulator for meteorological radiation[J]. Meteorological, Hydrological and Marine Instruments, 2018, 3: 32-35.

[20] PARUPUDI R V, SINGH H, KOLOKOTRONI M. Sun simulator for indoor performance assessment of solar photovoltaic cells[J]. Energy Procedia, 2019, 161: 376-338.